Local and regional drivers of environmental changes in two subtropical montane ponds (central China) over the last two centuries

Xu Chen[1*], Suzanne McGowan[2], Jia Peng[1], Ting Zheng[1], Xue Bai[1], Linghan Zeng[2]

1. State Key Laboratory of Biogeology and Environmental Geology, School of Geography and Information Engineering, China University of Geosciences, Wuhan 430074, China

2. School of Geography, University of Nottingham, Nottingham NG7 2RD, UK

[*]Corresponding author; e-mail address: xuchen@cug.edu.cn

HIGHLIGHTS

Primary producers of two subtropical montane ponds exhibited changes from the 1900s.

The drainage versus seepage hydrologies of each pond were important modulators of primary production.

Temperature and nitrogen deposition interacted with local catchment conditions to influence ecosystem response

Authors Contributions: XC and SM conceived and designed the study. XC, SM, JP, TZ, XB, and LZ collected and analysed the data. XC and SM wrote the manuscript.

Abstract: Central China, one of the Earth's distinctive ecoregions due to its endemic subtropical biota, has been subjected to enhanced nitrogen deposition and climate warming during recent decades. However, the extent and timescale of ecological changes are largely unexplored. Multiproxy analyses (diatoms, photosynthetic pigments and geochemistry) of ^{210}Pb-dated sediment cores from two shallow ponds within an alpine basin (central China) were used to investigate the response of primary producer communities to external stressors during the last two centuries. The study sites include one drainage pond and one seepage pond. Both ponds exhibited unambiguous changes in production and composition of photoautotrophs since the early 20th century, which are linked to climate warming, nitrogen deposition and local factors (e.g. lake morphometry, desiccation and macrophyte). Although primary producers responded to regional warming and nitrogen deposition, the ecological responses differed among ponds due to local factors. In the deeper seepage pond, light attenuation due to terrestrial organic matter input caused recent decreases in carotenoids and small fragilarioid taxa. In contrast, the co-occurrence of euterrestrial and tychoplanktonic diatoms in the shallower drainage pond was indicative of its hydrological instability. Our results indicate that subtropical montane ponds in the East Asian monsoon region appear to be strongly influenced by the combined effects of local (e.g. catchment-lake connectivity) and regional driving forces (e.g. warming and nitrogen deposition).

Key words: diatom; pigment; nitrogen deposition; climate warming; lake morphometry; palaeolimnology

INTRODUCTION

Montane lakes are remote aquatic ecosystems characterized by prolonged ice cover, short growing seasons, dilute water chemistry and low primary production (Catalan and others 2013; Wolfe and others 2013). As such, montane lakes may act as sentinels for a variety of environmental stressors, such as climate warming, hydrological alteration, and nitrogen deposition (Moser and others 2019). Algae, the dominant primary producers in aquatic ecosystems, are of global significance for biogeochemical cycling, and are an invaluable bioindicators of ongoing global change due to their wide distribution, high diversity, and sensitivity to habitat alteration (Rühland and others 2015). Local and regional driving forces may induce shifts in primary producers of montane water bodies, with substantial implications for higher trophic levels and ecosystem structure and function (Catalan and others 2013; Rühland and others 2015; Hobbs and others 2016).

A number of processes have been proposed as contributors to observed changes in primary producer communities of alpine lakes. Firstly, the elevated inorganic nitrogen concentrations due to atmospheric deposition has increased primary production in lakes (Bergström and Jansson 2006). Secondly, climate warming is proposed to enhance primary production by prolonging the growing season (Rühland and others 2015). Thirdly, changes in local factors, such as catchment-lake hydrological connection, are important driving forces for shifts in primary producers (Hu and others 2018; Moorhouse and others 2018; Hadley and others 2019). For example, vegetation and soil development can increase the influx of terrestrial coloured dissolved organic matter (CDOM) to lakes (McGowan and others 2018a), imposing a dual effect on primary producers, via nutrients (positively) and light (negatively) (Bergström and Karlsson 2019). Due to the complexities of these processes, the ecological responses of small

and shallow montane lakes may vary spatially and temporally (Catalan and others 2013; Rühland and others 2015).

Present knowledge on the effects of multiple stressors on primary producers mainly derives from Arctic, European and North American montane lakes (Binford and others1987; Caballero-Miranda 1996; Saros and others 2005; Catalan and others 2013; Rühland and others 2015; Hobbs and others 2016; Smol 2016; Moorhouse and others 2018), while there is a paucity of information on montane lakes in subtropical East Asia (Hu and others 2018; Wang and others 2020). Montane lakes are considered to be relatively pristine, nutrient-limited and seasonally frozen, and hence more sensitive to influxes of energy or mass from atmospheric changes (Vogt and others 2011; Smol 2016; Hadley and others 2019). Small and shallow lakes may show more pronounced biological responses to global environmental changes than deep lakes, due to their unique features of low water volumes and hydrological sensitivity resulting from high catchment: lake area ratios (Spaulding and others 2015; Rantala and others 2017; Giles and others 2018).

In monsoonal regions where rainfall patterns are generally intense and highly seasonal, the transfer of carbon and nutrients between the watershed and lake is likely to be highly efficient. However, the ecological responses of shallow lakes to eutrophication and hydrological changes are known to be complex because of strong benthic-pelagic interactions, which can result in distinctive macrophyte-dominated and turbid states (Squires and others 2002; Vadeboncoeur and others 2003; Scheffer and Jeppesen 2007). Long-term (millennial-scale) changes in lake level of montane lakes are associated with shifts in monsoonal cycles, and lake level variability has been linked to changes in ecosystem state in shallow lakes (REFS). Strong potential exists, therefore,

for abrupt ecosystem transitions in subtropical montane ponds which may be detectable in longer term records as recovered by palaeolimnology (Briddon and others 2020).

Recently there has been increasing interest in environmental changes in montane lakes of China (Hu and others 2014; Chen and others 2018; Yan and others 2018; Kang and others 2019). In northern China, Chen and others (2018) found that rising primary production was consistent with enhanced nitrogen deposition in a montane lake after the 1980s. In contrast, the responses of algal communities to atmospheric deposition are more muted in alpine lakes of southwestern China, probably mediated by catchment processes (Hu and others 2014, 2018; Kang and others 2019). Algal communities of deeper stratified lakes shift mainly due to weak mixing and strong stratification caused by warming in both northern and southern China (Chen and others 2014; Yan and others 2018). For achieving a deeper understanding of the combined effects of local and regional driving forces, there is a necessity to decipher the response of primary producer communities across a broader geographic area. Central China, located in the East Asian monsoon region with synchronous changes in seasonal rainfall and temperature, displays a rapid warming trend of 1.5 °C/100 years during the last century (Wang and others 2009). In Central China, nitrogen deposition is dominated by wet deposition and demonstrates the world's greatest increase rate (Ackerman and others 2019). The combination of local and regional drivers may cause substantial shifts in primary producer communities of montane lakes in central China.

In this study, we present fossil diatoms, preserved pigments and geochemical data ($\delta^{13}C$, $\delta^{15}N$, total organic carbon and total nitrogen) in sediment cores from two shallow but hydrologically different montane ponds (a seepage pond and a drainage pond with an outlet) in an alpine basin located in central China. Seepage ponds without surface outlets should enhance the accumulation of organic matter due to prolonged water

residence times, in comparison with drainage ponds (Spaulding and others 2015). We hypothesize that light attenuation due to enhanced CDOM accumulation in the slightly deeper seepage pond will inhibit the growth of some benthic algae, whereas primary producers (including macrophytes and phytobenthos) in the very shallow drainage pond would be free of light limitation and so probably more directly responsive to changing nutrient fluxes. The objectives of this study were to (1) investigate changes in primary producer communities of two montane ponds during the last two centuries; (2) evaluate potential effects of local (e.g. catchment-lake hydrological connectivity) and regional (e.g. climate warming, rainfall and nitrogen deposition) drivers on primary producer communities.

MATERIALS AND METHODS

Study area

Congping Basin (31°24′12″N, 110°03′25″E, 2080 m a.s.l.) is located in the Three Gorges Area (central China) that is a transition zone between the western mountains and the eastern plain of China (Fig. 1A). Bedrock within the basin is Triassic limestone, while the surrounding highlands feature Permian sandstone and sandy shale. The regional climate is strongly influenced by the subtropical monsoon, with cold, dry winters and cool, wet summers. There is a weather station at the nearby Dajiuhu Wetland (31°28′50″N, 110°00′09″E, 1758 m a.s.l.; 10 km away from Congping Basin). Mean annual air temperature is ~8℃, and mean annual precipitation is ~1700 mm at Dajiuhu weather station (Fig. 2a; Li and others 2019). According to the vertical lapse rate of temperature of 0.5 °C/100 m, air temperature at Congping would be ~1.5°C colder than at Dajiuhu. Mean monthly air temperature at Congping Basin is estimated to range from -6 °C to -2 °C between December and February (Fig. 2a), and hence water

bodies are ice-covered during the winter. Over the last century, temperature increased remarkably from the early 20th century, followed by a slight decrease until recent warming since the 1980s (Fig. 2b; Wang and others 2009). In contrast, seasonal precipitation displayed fluctuant trends over the last century, with an increasing trend in winter precipitation after 1980 (Fig. 2c). The mountains around the basin are characterized by montane conifers (e.g. *Pinus*, *Picea* and *Abies*), while the lowland vegetation within the basin is alpine meadow scattered with more than ten shallow ponds (Fig. 1B). The alpine meadow is dominated by *Carex*, *Allium* and *Sphagnum*. Surface soil in the basin is Alfisol, which is characterized by high proportions of SiO_2 (57%), Al_2O_3 (13%) and organic matter (18%, estimated by loss on ignition at 550°C), low contents of MgO (1.7%), CaO (0.6%) and Na_2O (0.8%), and relatively low pH (5.4) (Mo 2019).

These small ponds are developed from karst depressions, and there is no knowledge of these lakes drying within the last ~50 years. Humans have had relatively little direct effect on the landscape, with the exception of the expedition. Congping (CP) and Mulong (ML) ponds are selected as study sites (two unnamed ponds on published maps, Fig.1), and both of them are weakly-acidic, humic, oligotrophic, electrolyte-poor and fishless (Table 1). CP is a much shallower (20cm depth) drainage pond, covered with *Sparganium stoloniferum* (coverage of ~30%) with an outlet at the east, while ML is a deeper (1.5m depth) seepage pond with *Sphagnum* development around lake margins (Fig. 1).

Sample collection and laboratory analysis

Parallel sediment cores were retrieved from CP using a Russian corer in June 2016, and from ML using a Kajak gravity corer in September 2017, respectively. The gravity

corer was most suitable for collecting short cores from soft sediments in the deeper ML Pond. The length of sediment cores collected from CP and ML was 50 cm and 33 cm, respectively. The sediment cores were sectioned immediately in field at 1-cm intervals. The samples were stored at <4 °C until analysis; pigment sub-samples were stored frozen at -20 °C prior to laboratory analysis. Sediment samples were analysed for radioactive isotopes (^{210}Pb, ^{226}Ra and ^{137}Cs), total organic carbon (TOC), total nitrogen (TN), carbon and nitrogen isotopes, particle size spectra, diatoms and pigments.

The radioactivities of ^{210}Pb, ^{226}Ra and ^{137}Cs were measured at 2-cm intervals in ML and at 4-cm intervals in CP on a gamma spectrometer (Ortec HPGe GWL) following the procedures described in Appleby (2001). Following treatment with 10% HCl to remove carbonate, the samples were rinsed 3 times in distilled water and oven dried at 45°C. All dried samples were powdered in preparation for measurement of TOC, TN, δ^{13}C and δ^{15}N. TOC and TN were measured by combustion with an elemental analyser (vario EL cube), with reference to standard samples (precision of ±0.1%). δ^{13}C and δ^{15}N of organic matter were determined using a Thermo Fisher Scientific stable isotope mass spectrometer (DELTA V advantage), with reference to standard samples (precision of ±0.3‰). TOC, TN, δ^{13}C and δ^{15}N were analysed at intervals of every 2-cm. Measured δ^{13}C values were corrected for the Suess effect (the decrease in δ^{13}C of the atmosphere due to the release of CO_2 with low ^{13}C content by fossil fuel burning) following the polynomial correction factor described by Neumann and others (2002). Particle size spectra of samples were measured at 1-cm intervals using a Malven automated laser optical particle-size analyser (Mastersizer-3000) after the removal of carbonates by 10% HCl and organic matter by 30% H_2O_2.

Diatom samples were treated with HCl (10%) and H_2O_2 (30%) following the standard procedures (Battarbee and others 2001), and diatoms were counted using an

193 Olympus BX53 microscope with an oil immersion objective at 1000×. A minimum of
194 300 valves were counted in each sample. Diatom taxonomy mainly followed Krammer
195 and Lange-Bertalot (1986-1991). For pigment analyses, freeze-dried weighed
196 sediments (~ 200 mg) were extracted in a mixture of acetone: methanol: water (80: 15:
197 5) by leaving in a -20 °C freezer for 24 h. Extracts were filtered with a 0.22-μm-pore
198 PTFE filter, dried under N_2 gas, re-dissolved in an acetone: ion-pairing reagent:
199 methanol mixture (70: 25: 5) and then injected into an Agilent 1200 series high-
200 performance liquid chromatography unit. Pigments were identified and quantified
201 based on their retention time and absorption spectra, compared with pigment standards
202 (Leavitt and Hodgson 2001; McGowan 2013). To calculate pigment concentrations,
203 chromatogram peak areas were calibrated using commercial standards (DHI Denmark).
204 Linear regressions ($r > 0.99$) of mass pigment injected (as volume × concentration) and
205 peak area were used for calibration (Leavitt and Hodgson 2001). Lutein and zeaxanthin
206 did not separate in this study and so were reported here together. All concentrations
207 were expressed as nmol g^{-1} organic carbon.
208
209 **Data analysis**
210 Zonation schemes were developed for diatoms and pigments using the broken-stick
211 model (Bennett 1996) using stratigraphically constrained cluster analysis (CONISS) in
212 the Tilia program (Grimm 1991). Seasonal climate anomalies in the study area were
213 collected from Atlas of Seasonal Temperature and Precipitation Anomalies over China
214 (1880-2007) (Wang and others 2009). An early detrended correspondence analysis
215 (DCA) showed that the gradient lengths of the diatom and pigment data from both
216 ponds were less than 2 standard deviations, and hence principal component analysis
217 (PCA) was used to summarise the major trends and a linear model (redundancy analysis,

RDA) was used to reveal the correlations between primary producer communities and explanatory variables. Considering the uncertainty of the ^{210}Pb chronologies prior to ca. 1850 and the timescale of available paleoclimate data, only data from ca. 1880 were used in the RDAs. In the RDAs, diatoms and pigments were used as response variables, and the explanatory factors included TOC, TN, δ^{13}C, δ^{15}N, anomalies in seasonal temperature and precipitation. Forward selection, with the false discovery rate correction and the Monte Carlo tests ($p<0.05$, n=999 unrestricted permutations) was used to reduce the explanatory factors to those correlating significantly with response variables. Ordination analyses were performed using CANOCO 5.0 (Šmilauer and Lepš 2014).

RESULTS

Lithology and chronology

Sediments in the CP core consisted of grey silty gyttja between 50 and 40 cm, yellow-grey gyttja between 40 and 22 cm, yellow gyttja with many plant remains in the uppermost 22 cm. Sediments in the ML core were mainly composed of black gyttja, with many plant remains in the bottom layers (below 26 cm). Sedimentary particle size spectra, i.e. clay (< 4 μm), silt (4 - 64 μm) and sand (> 64 μm), are shown in Fig. 3. Sediments were dominated by silt and clay in the drainage pond CP, and by silt and sand in ML, the seepage pond. Concentrations of excess ^{210}Pb (^{210}Pb$_{ex}$) were calculated by subtracting the ^{226}Ra supported ^{210}Pb concentrations from the total ^{210}Pb activities (Appleby 2001). The ^{210}Pb$_{ex}$ profile is non-monotonic in both ponds (Fig. 3). One possible explanation is that hydrological changes due to monsoonal climate variability have influenced soil erosion and so sedimentation rates in these alpine ponds. Alterations in initial concentrations of ^{210}Pb and sedimentation rates indicate that both

243 the constant initial concentration (CIC) and constant flux constant sedimentation
244 (CFCS) models fail to yield a reliable chronology (Appleby 2001). The constant rate of
245 supply (CRS) allows changes in the initial concentrations and the sedimentation rates
246 at different layers, and hence the CRS model yields more realistic results than the CIC
247 and CFCS models (Appleby 2001). The ^{137}Cs activities reached a peak at 11.5 cm in
248 CP core (Fig. 3a) and at 12.5 cm in ML core (Fig. 3b), which can be assigned to the
249 1963 maximum atmospheric global fallout as a result of nuclear weapons testing
250 (Appleby 2001). In order to improve the accuracy of the chronology, the ^{137}Cs 1963
251 peak was used as an independent dated reference level. The final age-depth model was
252 calculated using the CRS model, together with the ^{137}Cs 1963 peak as a reference level.
253 Mass accumulation rate (MAR) in CP core increased to a peak around the 1880s, and
254 reached consistently low rates from the 1970s onwards after a visible decrease between
255 the 1880s and the 1970s. In contrast, MAR in ML core displayed a rising trend toward
256 the core tops.
257
258 **Diatom stratigraphy**
259 Over 143 diatom taxa were identified from the two sediment cores, with a relatively
260 high species richness of taxa which prefer oligotrophic conditions. The diatom
261 assemblages were dominated by benthic taxa, such as *Staurosira construens* var. *venter*
262 (Ehrenberg) Hamilton, *Navicula cryptotenella* Lange-Bertalot, *Sellaphora pupula*
263 (Kützing) Mereschkowsky, and *Pinnularia microstauron* (Ehrenberg) Cleve, with
264 frequent occurrences of *Aulacoseira alpigena* (Grunow) Krammer (Fig. 4). The two
265 ponds had different taxonomic and temporal changes in diatom composition, in spite of
266 their adjacent locations.

In CP, diatom assemblages were characterized by euterrestrial species before ca.1910 (Fig. 4a), such as *Hantzschia amphioxys* (Ehrenberg) Grunow and *Pinnularia borealis* Ehrenberg. The most pronounced changes occurred between 1910 and 1922, with the replacement of euterrestrial species by opportunistic species (i.e. *S. construens* var. *venter* and *Achnanthidium minutissimum* (Kützing) Czarnecki). Between 1922 and 1980, *A. alpigena*, *Cymbopleura naviculiformis* (Auerswald) Krammer, *Eunotia mucophila* (Lange-Bertalot et Nörpel) Lange-Bertalot increased gradually at the expense of a visible decrease in *S. construens* var. *venter*. The subdominant species *Gomphonema parvulum* (Kützing) Kützing and *S. pupula* increased to a peak at around 1930, and gradually decreased thereafter. After 1980, diatom communities were co-dominated by *S. construens* var. *venter* and *A. alpigena*, and remained relatively stable.

In ML, epiphytic or epipelic species were dominant throughout the record, including *S. construens* var. *venter*, *N. cryptotenella*, *S. pupula* and *P. microstauron* (Fig. 4b). After 1955, epiphytic diatoms increased towards the core tops, such as *Brachysira brebissonii* Ross, *Eunotia bilunaris* (Ehrenberg) Schaarschmidt and *Eunotia exigua* (Brébisson) Rabenhorst. *S. construens* var. *venter* remained the dominant species, despite its recent decrease. The subdominant species *N. cryptotenella* increased to a peak at around 1963, followed by a gradual decrease.

Pigment stratigraphy

In CP, all pigments exhibited similar patterns with low concentrations before 1925. Thereafter they all began to increase, with further visible increases after 1960 (Fig.5a). In ML, there were two obvious shifts in pigment composition (Fig. 5b). Before 1948, pigment composition was characterized by high concentrations of alloxanthin (cryptophytes), fucoxanthin and diatoxanthin (siliceous algae), lutein-zeaxanthin (from

292 plants, chlorophytes and cyanobacteria), pheophytin *b* (plants and chlorophytes),
293 pheophorbide *a* (grazing or degradation of Chl *a*). Lutein-zeaxanthin increased to a
294 peak between 1948 and 1980, concurrent with relatively stable concentrations of other
295 pigments. Chl *a* and Chl *b* increased exponentially after 1980, with concurrent
296 decreases in carotenoid pigments.
297
298 **Geochemistry records**
299 The changing TOC and TN contents are accompanied by significant variations in
300 the isotopic composition of organic matter (Fig. 6). Sedimentary $\delta^{15}N$ values became
301 significantly lighter towards the sediment surface in the two lakes, i.e. from 0.3‰ to -
302 1.5‰ in ML and from 6.4‰ to 1.6‰ in CP. Sedimentary TN showed a linear increase
303 in both lakes after the 1900s, especially a recent acceleration since the 1980s. The
304 Suess-corrected $\delta^{13}C$ changed in the opposite directions in the two lakes, i.e. an increase
305 in ML but a decrease in CP. TOC gradually increased by ca. 10% in CP, whereas it
306 decreased slightly before the 1970s, followed by a rebound in ML. The molar ratios of
307 carbon to nitrogen (C/N) ranged from 11 to 20 in both lakes. C/N ratios in CP were
308 variable, but generally increased before 1960 and decreased thereafter; while the ratios
309 were more stable and exhibited a gradual decrease in ML.
310
311 **Multivariate analysis**
312 In CP, diatom PCA 1 and pigment PCA 1 captured 47% and 81% of the total
313 variance in diatoms and pigments, respectively. Diatom PCA 1 represented a shift from
314 euterrestrial (e.g. *H. amphioxys* and *P. borealis*) to aquatic taxa, while all the pigment
315 types were positively correlated with pigment PCA 1. In ML, diatom PCA 1 and
316 pigment PCA 1 explained 64% and 40% of the total variance in diatoms and pigments,

317 respectively. Diatom PCA 1 was most strongly correlated with changes in small
318 fragilarioid and moss-attached taxa, while pigment PCA 1 in ML was positively
319 correlated with changes in chlorophylls. Diatom and pigment PCA 1 sample scores of
320 the two lakes displayed obvious changes from the early 1900s, broadly corresponding
321 to the $\delta^{15}N$ depletion in the two sediment cores, the nitrate enrichment in the Himalayan
322 ice core (Thompson and others 2000), the rising nitrogen content and the $\delta^{15}N$ (NO_3^-)
323 depletion in the Greenland ice core (Geng and others 2014) (Fig. 7). In the RDA
324 analyses of environment-diatom and -pigment correlations at CP and ML ponds, both
325 diatom and pigment assemblages were significantly correlated with seasonal
326 temperature and $\delta^{15}N$ but not with changes in total annual rainfall (Fig. 8).
327
328 **DISCUSSION**
329 The Congping basin receives water from the surrounding mountains (local relief ca.
330 300m) and is an interconnected mosaic of alpine meadows, wetlands and ponds. Such
331 heterogeneity is driven by localised conditions across the basin and is important in
332 supporting terrestrial and aquatic biodiversity of this region (Chen and others 2012).
333 Our results indicate different conditions in water bodies located within a few hundred
334 metres of one another. Although primary producers responded to the same regional
335 drivers of nitrogen deposition and warming, the ecological consequences differed
336 among ponds (Fig. 9). Differences in hydrological setting, water depth and macrophyte
337 communities between the drainage and seepage ponds are useful in helping to
338 understand the divergent ecological responses.
339
340 **Lake-specific factors**

Before the 1900s, high abundances of euterrestrial diatom species (e.g. *H. amphioxys* and *P. borealis*) were concomitant with occasional occurrence of tychoplanktonic species (i.e. *A. alpigena*) in the very shallow drainage pond CP, suggesting that it was ephemeral (seasonally dried out) during the dry season (winter), with episodic flooding and water-level rises in the wet season (summer). The near absence of pigments apart from alteration products of chlorophylls *a* and *b* (pheophytin *a* and *b*) corroborates the idea of seasonal desiccation because exposure to oxygen and light accelerates pigment degradation (Leavitt and Hodgson 2001). A seasonally desiccated wetland would most likely be dominated by wetland plants such as sedges, rushes and mosses which produce chlorophylls *a* and *b*, consistent with the pheo-pigments recorded. Due to water table drawdown in the dry season and wind-driven mixing, kinetic isotope fraction during protein hydrolysis likely contributed to the ^{15}N-enrichment in oxic conditions (Lehmann and others 2002) before the 1900s. Our evidence suggests, therefore, that there were pronounced hydrological changes in CP, the drainage pond, from ephemeral to more permanently inundated after the 1900s, leading to a rise in the production and preservation of algae-derived carotenoids more commonly associated with shallow freshwater communities (McGowan 2013).

The pronounced increase in temperature at this time (Fig. 2b) could be associated with this shift in hydrology. Warmer temperatures can promote the development of vegetation and soil, which could act as giant sponges retaining moisture during the rainy season and steadily supplying water to the ponds during the dry season (Giles and others 2018). This could buffer against increased evapotranspiration caused by higher temperatures. Vegetation growth may also restrict drainage pathways, increasing the residence time of the pond, indicating the potential for localised geomorphic effects within the basin (Gurnell 2014). Local changes in hydrology most likely explain the

non-significant relationship between rainfall and pigment responses (Fig. 8). Rising abundance of *A. alpigena* in CP after the 1930s indicated an increase in water depth (Fig. 4); in particular, the subdominance of *A. alpigena* and low C/N ratios after the 1980s indicated a status of permanent inundation during the ice-free season. Hydrological changes were also evidenced by an increase in coarse particles (Fig. 3). The coarsening grain size may indicate fine suspended particles would be washed out, as rising water levels caused water discharge through the outlet (Fig. 1).

In contrast to CP, the deeper seepage pond ML displayed clear decreases in carotenoid pigments and small fragilarioid taxa (i.e. *S. construens* var. *venter*) after the 1980s (Figs. 4 and 5). Recent changes in diatom assemblages were significantly correlated with higher $\delta^{13}C$ (Fig. 8b), suggestive of a linkage to carbon cycling. The ranges of Suess-corrected $\delta^{13}C$ (between -29.7‰ and -25.7‰) and C/N ratios (from 11 to 20) in both ponds are within the range of allochthonous soil organic matter (Meyers and Teranes 2001) and C3 plants (e.g. *Carex* and *Sphagnum*) in the nearby Dajiuhu Wetland ($\delta^{13}C$ ranging from -29.3‰ to -22.8‰; Liu and others 2018), suggesting that organic matter is mainly sourced from terrigenous inputs, with some contributions from algae. In ML, an increase in $\delta^{13}C$ after the early 1900s may imply that littoral *Sphagnum* made a larger contribution to the carbon pool, since *Sphagnum* mosses have relatively heavier $\delta^{13}C$ values than other plants (e.g. *Juncus*, *Polytrichum* and *Sanguisorba*) (Liu and others 2018).

Continuous inputs of CDOM attenuate light and may restrict light penetration and inhibit benthic primary productivity (McGowan and others 2018a; Bergström and Karlsson 2019). Higher sedimentary TN and TOC contents in the seepage pond ML may suggest enhanced organic matter accumulation (Fig. 6). Shallowing of the euphotic zone due to terrestrial CDOM inputs, may thus have impeded the growth of benthic

391 algae beneath the euphotic zone (Fig. 9). This is consistent with recent decreases in
392 fossil carotenoids and small fragilarioid species after 1955. After 1980, changes to more
393 diverse periphytic taxa that are associated with littoral habitats and mossy substrates
394 (e.g. *Brachysira*, *Frustulia* and *Eunotia* species) (Chen and others 2016), are inferred
395 to reflect increased littoral habitat availability with longer growing seasons. Such shifts
396 were not observed in CP because CDOM additions could not have a significant effect
397 on light attenuation at the bottom of such a shallow pond (20cm depth).

398 Differences among the pond diatom assemblages are consistent with the
399 hydrological characteristics. For example, *A. minutissimum* and the planktonic *A.*
400 *alpigena* successively increased in the drainage pond CP since water level increased,
401 and are common in snowmelt-fed Swiss alpine basins, whereas *T. flocculosa* was
402 present in the seepage pond ML and may be more common in lakes which are
403 disconnected from riverine influence (Robinson and Kawecka 2005). The diatom
404 assemblages of both ponds were dominated by benthic taxa, including some motile
405 species (e.g. *N. cryptotenella*, *S. pupula*, *P. microstauron* and *A. minutissimum*) that
406 can migrate within biofilms (McGowan and others 2018b). Migration of motile diatoms
407 enables the avoidance of unfavourable conditions (e.g. desiccation, excessive light
408 exposure, grazing and nutrient limitation), to maximise overall fitness and productivity
409 of the biofilm (Consalvey and others 2004).

410 Nutrients may be delivered in pulses to lake margins during snowmelt, which may
411 offer benthic diatoms living at lake margins a competitive advantage over planktonic
412 taxa in these seasonally frozen ponds (McGowan and other 2018b). However, in this
413 region summer monsoon rains deliver the majority of rainfall, supplying benthic
414 diatoms with a regular supply of catchment-delivered nutrients (Hu and others 2018).
415 The majority of the benthic taxa in both ponds would be considered epipelic or

periphytic species, suggesting that shifts in the diatom assemblages in the ponds were not strongly associated with changes in macrophyte abundance (Scheffer and Jeppesen 2007), but instead driven by changes in water level and nutrients in the drainage pond CP where light was not limiting, and water browning and seasonal water level fluctuations in the seepage pond ML where the relative availability of benthic: pelagic habitat was regulated by light limitation.

The linkage to climate variability

Pigment and diatom data were significantly correlated with seasonal temperature, but not with rainfall in both ponds (Fig. 8), suggesting that climate warming stimulates changes in primary producer communities. In shallow water bodies, light penetration to the bottom allows the development of complex benthic communities which respond to warming differently (Spaulding and others 2015). The increasing primary production (inferred from chlorophylls and their derivatives) in both ponds in the early 1900s was compatible with a persistent rise in regional temperature between 1900 and 1920 (Figs. 5 and 7). The shortened ice-cover duration under warmer climate is an important factor influencing the growth of primary producers in the study ponds (Fig. 9). Firstly, a longer ice-free season would enhance the terrestrial-aquatic linkage (i.e. runoff and nutrients from land to lake). Secondly, a longer growing season allows more time for the development of primary producer communities, including macrophytes which provide substrates for epiphytes, thus accelerating annual biomass accumulation (Rühland and others 2015). Taken together, warming-related processes may promote primary production of the study ponds, indicated by rising pigment concentrations in the early 1900s.

Seasonal precipitation was not significantly correlated with pigments and diatoms of both ponds, indicating that precipitation effects were probably mediated by local hydrological factors. For example, groundwater is an important component of the water cycle in limestone areas, and there are lags between rainfall and groundwater recharge which may have been particularly important in the seepage lake (ML). In contrast, it appears that local vegetation development might have influenced the drainage of CP and increased the complexity of the relationship between rainfall and ecological response. For example, lower rainfall before the 1900s probably caused periodic desiccation, subsequently increasing phosphorus availability by mineralization processes of inorganic and organic phosphorus in lake sediment (Reddy and other 2005). An increasing supply of soluble phosphorus would facilitate the growth of eutrophic species (e.g. *C. naviculiformis*, *G. parvulum*, *Stauroneis phoenicenteron* Nitzsch) (cf. Van Dam and others 1994) in CP Pond (Fig. 4a). In addition, an increase in winter rainfall after the 1980s (Fig. 2c) would provide habitats suited to small fragilarioid taxa that can compete well under ice during the winter (Laing and Smol 2000; Lotter and Bigler 2000). This explanation probably accounted for the proliferation of *S. construens* var. *venter* in the upper strata of CP core (Fig. 4a).

The linkage to nitrogen enrichment

Sediment $\delta^{15}N$ has declined progressively in both lakes since the early 20th century, and, despite considerable local heterogeneity and ecological complexity in these ponds, this trend parallels the records of nitrogen deposition observed in other remote Northern Hemisphere lakes (Holtgrieve and others 2011), a Himalayan ice core (Thompson and others 2000), and the Greenland Ice Sheet (Geng and others 2014) (Fig. 7). Although fertilizer use was limited before 1950, inputs from animal manure from the fast-growing

animal stocks, and human excreta from the expanding population have increased during the early 20th century (Bouwman and others 2013). Average nitrogen deposition rates over forests in East Asia have increased from less than 2 kg N ha^{-1} yr^{-1} in the mid-19th century to more than 3 kg N ha^{-1} yr^{-1} in the mid-20th century (Wang and others 2017). Remote montane lakes are often N-limited, which renders them susceptible to the enrichment effects of nitrogen deposition (Bergström and Jansson 2006; Baron and others 2011). Enhanced nitrogen deposition elicits mesotrophic species as N-deposition rates cross a critical load (Saros and others 2011).

Carotenoids (e.g. lutein-zeaxanthin) increased gradually in both ponds from the 1920s (Fig. 5), suggesting that rising N inputs may have caused nutrient enrichment with higher primary production. Meanwhile, synchronous increases in chlorophylls and their derivatives (e.g. Chl *a* and pheophytin *a*) implied that nutrient enrichment might also promote the growth of macrophytes that contain chlorophylls and their derivatives (McGowan 2013). However, gradual decreases in carotenoids in the seepage pond ML after the 1980s indicated that algal growth might be inhibited by local factors (Fig. 9). Meanwhile, nutrient inputs promoted the development of aquatic plants in the littoral zone, probably accounting for rising concentrations of chlorophylls and their derivatives in ML Pond (McGowan 2013). Although most dominant diatom taxa in both ponds are thought to use inorganic forms of nitrogen, some taxa that can utilise organically bound nitrogen increased obviously after the early-1900s (Tuchman and others 2006), such as the increase of *E. mucophila*, *S. pupula* and *C. naviculiformis* in CP, and the expansion of *E. exigua* and *E. bilunaris* in ML.

CONCLUSIONS

This study investigates the response of primary producer communities to local and regional driving forces in two subtropical montane ponds (central China) during the last two centuries. Climate warming and nitrogen deposition have altered biomass and community composition of primary producers, probably mediated by local factors (e.g. lake morphometry and catchment-lake connections). Further warming and nitrogen deposition would possibly increase autotrophic biomass (especially nitrophilous taxa) in these subtropical montane ponds, probably influencing ecosystem structure and function through aquatic food web. The effects of warming and nitrogen deposition on primary producers are mainly deduced from correlational statistical analyses, and previous knowledge of the autoecology of dominant taxa. In order to disentangle the effects of warming and nitrogen deposition, further seasonal monitoring of primary producers are needed in the study region. Therefore, it is essential to conduct palaeolimnological and seasonal monitoring studies in order to track the ecological responses of subtropical montane lakes to changes in local and regional drivers over subtropical East Asia.

ACKNOWLEDGEMENTS

This study was funded by the National Natural Science Foundation of China (41572343). We acknowledge Teresa Needham, Zhang Zhiqi, Huang Xianyu, Qiao Qianglong, Zhang Yiming, Zhang Zhou, Liang Jia, Xia Weilan, Song Huyue, Ji Junliang, Jiang ying and Ji Jing for field and laboratory assistance. We are grateful to anonymous reviewers and the subject-matter editor Dr. James Elser for their constructive comments. This work is dedicated affectionately to Xu's father Mr. Chen Xianci.

514 **REFERENCES**

515 Ackerman D, Millet DB, Chen X. 2019. Global Estimates of Inorganic Nitrogen
516 Deposition Across Four Decades. Global Biogeochemical Cycles 33: 1-8.

517 Appleby PG. 2001. Tracking Environmental Change Using Lake Sediments. Last W,
518 Smol J. (eds), pp. 171-203, Springer Netherlands.

519 Baron JS, Driscoll CT, Stoddard JL, Richer EE. 2011. Empirical Critical Loads of
520 Atmospheric Nitrogen Deposition for Nutrient Enrichment and Acidification of
521 Sensitive US Lakes. Bioscience 61: 602-613.

522 Battarbee RW, Jones VJ, Flower RJ, Cameron NG, Bennion H, Carvalho L, Juggins S.
523 2001. Tracking Environmental Change Using Lake Sediments. Smol JP, Birks HJB,
524 Last WM, Bradley RS, Alverson K. (eds), pp. 155-202, Springer Netherlands.

525 Bennett KD. 1996. Determination of the number of zones in a biostratigraphical
526 sequence. New Phytologist 132: 155-170.

527 Bergström AK, Jansson M. 2006. Atmospheric nitrogen deposition has caused nitrogen
528 enrichment and eutrophication of lakes in the northern hemisphere. Global Change
529 Biology 12: 635-643.

530 Bergström AK, Karlsson J. 2019. Light and nutrient control phytoplankton biomass
531 responses to global change in northern lakes. Global Change Biology 25: 2021-2029.

532 Binford MW, Brenner M, Whitmore TJ, Higuera-Gundy A, Deevey ES, Leyden B.
533 1987. Ecosystems, paleoecology and human disturbance in subtropical and tropical
534 America. Quaternary Science Reviews 6: 115-128.

535 Bouwman L, Goldewijk KK, Van Der Hoek KW, Beusen AHW, Van Vuuren DP,
536 Willems J, Rufino MC, Stehfest E. 2013. Exploring global changes in nitrogen and
537 phosphorus cycles in agriculture induced by livestock production over the 1900–
538 2050 period. Proceedings of the National Academy of Sciences 110: 20882.

539 Briddon C, McGowan S, Metcalfe S, Panizzo V, Lacey J, Engels S, Leng M, Mills K,
540 Shafiq M, Idris M. 2020. Diatoms in a sediment core from a flood pulse wetland in
541 Malaysia record strong responses to human impacts and hydro‐climate over the
542 past 150 years. Geo: Geography and Environment 7.
543 Caballero-Miranda M. 1996. The diatom flora of two acid lakes in central Mexico.
544 Diatom Research 11: 227-240.
545 Catalan J, Pla-Rabés S, Wolfe A, Smol J, Rühland K, Anderson NJ, Kopáček J, Stuchlík
546 E, Schmidt R, Koinig K, Camarero L, Flower R, Heiri O, Kamenik C, Korhola A,
547 Leavitt P, Psenner R, Renberg I. 2013. Global change revealed by
548 palaeolimnological records from remote lakes: a review. Journal of Paleolimnology
549 49: 513-535.
550 Chen J, Liu J, Xie C, Chen G, Chen J, Zhang Z, Zhou A, Rühland KM, Smol JP, Chen
551 F. 2018. Biogeochemical responses to climate change and anthropogenic nitrogen
552 deposition from a ~200-year record from Tianchi Lake, Chinese Loess Plateau.
553 Quaternary International 493: 22-30.
554 Chen C, Zhao L, Zhu C, Wang J, Jiang J, Yang S. 2014. Response of diatom community
555 in Lugu Lake (Yunnan–Guizhou Plateau, China) to climate change over the past
556 century. Journal of Paleolimnology 51: 357-373.
557 Chen D, Xiao W, Shao L, Zheng W, Liu T, He H, Chen, L. 2012. Spermatophyte flora
558 of Wulipo Nature Reserve of Wushan County, Chongqing City. Journal of Huazhong
559 Agricultural University 31: 303-312.
560 Chen X, Bu Z, Stevenson MA, Cao Y, Zeng L, Qin B. 2016. Variations in diatom
561 communities at genus and species levels in peatlands (central China) linked to
562 microhabitats and environmental factors. Science of the Total Environment 568:
563 137-146.

564 Consalvey M, Paterson DM, Underwood GJC. 2004. The ups and downs of life in a
565 benthic biofilm: migration of benthic diatoms. Diatom Research 19: 181-202.
566 Geng L, Alexander B, Cole-Dai J, Steig EJ, Savarino J, Sofen ED, Schauer AJ. 2014.
567 Nitrogen isotopes in ice core nitrate linked to anthropogenic atmospheric acidity
568 change. Proceedings of the National Academy of Sciences 111: 5808.
569 Giles MP, Michelutti N, Grooms C, Smol JP. 2018. Long-term limnological changes in
570 the Ecuadorian páramo: Comparing the ecological responses to climate warming of
571 shallow waterbodies versus deep lakes. Freshwater Biology 63: 1316-1325.
572 Grimm E. 1991. TILIA version 1.11. TILIAGRAPH version 1.18. A Users Notebook.
573 Illinois State Museum, Springfield, USA.
574 Gurnell A. 2014. Plants as river system engineers. Earth Surface Processes and
575 Landforms 39: 4-25.
576 Hadley KR, Paterson AM, Rühland KM, White H, Wolfe BB, Keller W, Smol JP. 2019.
577 Biological and geochemical changes in shallow lakes of the Hudson Bay Lowlands:
578 a response to recent warming. Journal of Paleolimnology 61: 313-328.
579 Hobbs WO, Lafrancois BM, Stottlemyer R, Toczydlowski D, Engstrom DR, Edlund
580 MB, Almendinger JE, Strock KE, VanderMeulen D, Elias JE, Saros JE. 2016.
581 Nitrogen deposition to lakes in national parks of the western Great Lakes region:
582 Isotopic signatures, watershed retention, and algal shifts. Global Biogeochemical
583 Cycles 30: 514-533.
584 Holtgrieve GW, Schindler DE, Hobbs WO, Leavitt PR, Ward EJ, Bunting L, Chen G,
585 Finney BP, Gregory-Eaves I, Holmgren S, Lisac MJ, Lisi PJ, Nydick K, Rogers LA,
586 Saros JE, Selbie DT, Shapley MD, Walsh PB, Wolfe AP. 2011. A Coherent
587 Signature of Anthropogenic Nitrogen Deposition to Remote Watersheds of the
588 Northern Hemisphere. Science 334: 1545.

589 Hu Z, Anderson NJ, Yang X, McGowan S. 2014. Catchment-mediated atmospheric
590 nitrogen deposition drives ecological change in two alpine lakes in SE Tibet. Global
591 Change Biology 20: 1614-1628.
592 Hu Z, Yang X, Anderson NJ, Li Y. 2018. The Landscape–Atmosphere Continuum
593 Determines Ecological Change in Alpine Lakes of SE Tibet. Ecosystems 21: 839-
594 851.
595 Kang W, Chen G, Wang J, Huang L, Wang L, Li R, Hu K, Liu Y, Tao J, Blais JM,
596 Smol JP. 2019. Assessing the impact of long-term changes in climate and
597 atmospheric deposition on a shallow alpine lake from southeast Tibet. Science of the
598 Total Environment 650: 713-724.
599 Krammer K, Lange-Bertalot H. (eds) (1986-1991) Bacillariophyceae., Gustav Fischer
600 Verlag, Stuttgart/Jena.
601 Laing TE, Smol JP. 2000. Factors influencing diatom distributions in circumpolar
602 treeline lakes of northern Russia. Journal of Phycology 36: 1035-1048.
603 Leavitt P, Hodgson D. 2001. Tracking Environmental Change Using Lake Sediments.
604 Smol J, Birks HJ, Last W, Bradley R, Alverson K. (eds), pp. 295-325, Springer
605 Netherlands.
606 Lehmann MF, Bernasconi SM, Barbieri A, McKenzie JA. 2002. Preservation of organic
607 matter and alteration of its carbon and nitrogen isotope composition during simulated
608 and in situ early sedimentary diagenesis. Geochimica et Cosmochimica Acta 66:
609 3573-3584.
610 Li JQ, Ge JW, Peng FJ, Li YY, Zhou Y, Li YF, Weng WC. 2019. Studies on carbon-
611 water flux and water use efficiency in Dajiuhu Peat Wetland Ecosystem. Safety and
612 Environmental Engineering 26: 14-25.

Liu J, Chen Y, Ma L, Pu H, Liu C, Zhao Z., Shu Q. 2017. The $\delta^{13}C$ of cellulose from modern plants and its responses to the atmosphere – From the peatland records of Dajiuhu, China. The Holocene 28(3): 408-414.

Lotter AF, Bigler C. 2000. Do diatoms in the Swiss Alps reflect the length of ice-cover? Aquatic Sciences 62: 125-141.

McGowan S. 2013. Encyclopedia of Quaternary Science (Second Edition). Elias SA, Mock CJ. (eds), pp. 326-338, Elsevier, Amsterdam.

McGowan S, Anderson NJ, Edwards ME, Hopla E, Jones V, Langdon PG, Law A, Soloveiva N, Turner S, van Hardenbroek M, Whiteford EJ, Wiik E. 2018a. Vegetation transitions drive the autotrophy-heterotrophy balance in Arctic lakes. Limnology and Oceanography Letters 3: 246-255.

McGowan S, Gunn HV, Whiteford EJ, Anderson NJ, Jones VJ, Law AC. 2018b. Functional attributes of epilithic diatoms for palaeoenvironmental interpretations in South-West Greenland lakes. Journal of Paleolimnology 60: 273-298.

Meyers PA, Teranes JL. 2001. Tracking Environmental Change Using Lake Sediments: Physical and Geochemical Methods. Last WM, Smol JP. (eds), pp. 239-269, Springer Netherlands, Dordrecht.

Mo R. 2019. The characteristics of elemental composition of soil in alpine basins in the Middle Yangtze reaches-a case study in Dajiuhu and Congping, China University of Geosciences (Wuhan), Wuhan.

Moorhouse HL, McGowan S, Taranu ZE, Gregory-Eaves I, Leavitt PR, Jones MD, Barker P, Brayshaw SA. 2018. Regional versus local drivers of water quality in the Windermere catchment, Lake District, United Kingdom: The dominant influence of wastewater pollution over the past 200 years. Global Change Biology 24: 4009-4022.

637 Moser KA, Baron JS, Brahney J, Oleksy IA, Saros JE, Hundey EJ, Sadro SA, Kopacek
638 J, Sommaruga R, Kainz MJ, Strecker AL, Chandra S, Walters DM, Preston DL,
639 Michelutti N, Lepori F, Spaulding SA, Christianson KR, Melack JM, Smol JP. 2019.
640 Mountain lakes: Eyes on global environmental change. Global and Planetary Change
641 178: 77-95.
642 Neumann T, Stögbauer A, Walpersdorf E, Stüben D, Kunzendorf H. 2002. Stable
643 isotopes in recent sediments of Lake Arendsee, NE Germany: response to
644 eutrophication and remediation measures. Palaeogeography, Palaeoclimatology,
645 Palaeoecology 178: 75-90.
646 Rantala MV, Luoto TP, Weckström J, Rautio M, Nevalainen L. 2017. Climate drivers
647 of diatom distribution in shallow subarctic lakes. Freshwater Biology 62: 1971-1985.
648 Reddy KR, Wetzel RG, Kadlec RH. 2005. Biogeochemistry of Phosphorus in Wetlands.
649 Phosphorus: Agriculture and the Environment: 263-316.
650 Robinson CT, Kawecka B. 2005. Benthic diatoms of an Alpine stream/lake network in
651 Switzerland. Aquatic Sciences 67: 492-506.
652 Rühland K, Paterson A, Smol J. 2015. Lake diatom responses to warming: reviewing
653 the evidence. Journal of Paleolimnology 54: 1-35.
654 Saros JE, Clow DW, Blett T, Wolfe AP. 2011. Critical Nitrogen Deposition Loads in
655 High-elevation Lakes of the Western US Inferred from Paleolimnological Records.
656 Water, Air, & Soil Pollution 216: 193-202.
657 Saros JE, Michel TJ, Interlandi SJ, Wolfe AP. 2005. Resource requirements of
658 *Asterionella formosa* and *Fragilaria crotonensis* in oligotrophic alpine lakes:
659 implications for recent phytoplankton community reorganizations. Canadian Journal
660 of Fisheries and Aquatic Sciences 62: 1681-1689.
661 Scheffer M, Jeppesen E. 2007. Regime Shifts in Shallow Lakes. Ecosystems 10: 1-3.

662 Šmilauer P, Lepš J. 2014. Multivariate Analysis of Ecological Data using CANOCO 5,
663 Cambridge University Press, Cambridge.
664 Smol JP. 2016. Arctic and Sub-Arctic shallow lakes in a multiple-stressor world: a
665 paleoecological perspective. Hydrobiologia 778: 253-272.
666 Spaulding SA, Otu MK, Wolfe AP, Baron JS. 2015. Paleolimnological Records of
667 Nitrogen Deposition in Shallow, High-Elevation Lakes of Grand Teton National
668 Park, Wyoming, U.S.A. Arctic, Antarctic, and Alpine Research 47: 703-717.
669 Squires MM, Lesack LFW, Huebert D. 2002. The influence of water transparency on
670 the distribution and abundance of macrophytes among lakes of the Mackenzie Delta,
671 Western Canadian Arctic. Freshwater Biology 47: 2123-2135.
672 Thompson LG, Yao T, Mosley-Thompson E, Davis ME, Henderson KA, Lin PN. 2000.
673 A High-Resolution Millennial Record of the South Asian Monsoon from Himalayan
674 Ice Cores. Science 289: 1916.
675 Tuchman NC, Schollett MA, Rier ST, Geddes P. 2006. Advances in Algal Biology: A
676 Commemoration of the Work of Rex Lowe. Stevenson RJ, Pan Y, Kociolek JP,
677 Kingston JC. (eds), pp. 167-177, Springer Netherlands, Dordrecht.
678 Vadeboncoeur Y, Jeppesen E, Zanden MJV, Schierup HH, Christoffersen K, Lodge
679 DM. 2003. From Greenland to green lakes: Cultural eutrophication and the loss of
680 benthic pathways in lakes. Limnology and Oceanography 48: 1408-1418.
681 Van Dam H, Mertens A, Sinkeldam J. 1994. A coded checklist and ecological indicator
682 values of freshwater diatoms from The Netherlands. Netherlands Journal of Aquatic
683 Ecology 28: 117-133.
684 Vogt RJ, Rusak JA, Patoine A, Leavitt PR. 2011. Differential effects of energy and
685 mass influx on the landscape synchrony of lake ecosystems. Ecology 92: 1104-1114.

686 Wang R, Goll D, Balkanski Y, Hauglustaine D, Boucher O, Ciais P, Janssens I,
687 Penuelas J, Guenet B, Sardans J, Bopp L, Vuichard N, Zhou F, Li B, Piao S, Peng
688 S, Huang Y, Tao S. 2017. Global forest carbon uptake due to nitrogen and
689 phosphorus deposition from 1850 to 2100. Global Change Biology 23: 4854-4872.
690 Wang R, Hu Z, Wang Q, Xu M, Zheng W, Zhang K, Yang X. 2020. Discrepancy in the
691 responses of diatom diversity to indirect and direct human activities in lakes of the
692 southeastern Tibetan Plateau, China. Anthropocene 30, 100243.
693 Wang SW, Zhao ZG, Li WJ. 2009. Atlas of Seasonal Temperature and Precipitation
694 Anomalies over China (1880-2007), China Meteorological Press, Beijing.
695 Wolfe AP, Hobbs WO, Birks HH, Briner JP, Holmgren SU, Ingólfsson Ó, Kaushal SS,
696 Miller GH, Pagani M, Saros JE, Vinebrooke RD. 2013. Stratigraphic expressions of
697 the Holocene–Anthropocene transition revealed in sediments from remote lakes.
698 Earth-Science Reviews 116: 17-34.
699 Yan Y, Wang L, Li J, Li JJ, Zou YF, Zhang JY, Li P, Liu Y, Xu B, Gu ZY, Wan XQ.
700 2018. Diatom response to climatic warming over the last 200 years: A record from
701 Gonghai Lake, North China. Palaeogeography Palaeoclimatology Palaeoecology
702 495: 48-59.

TABLE AND FIGURE CAPTIONS

Table 1 Summaries of environmental conditions in the two study ponds.

Figure 1 Maps showing the location of study sites in Asia (A) and local topography (B), and photos of Congping (C) and Mulong (D) ponds. The inserted maps in Figure B show local topography of Congping (the upper) and Mulong (the lower). Congping is dominated by *Sparganium stoloniferum*, with coverage of ~30%. Maps A and B have been modified from the maps downloaded from http://www.lib.utexas.edu/maps/asia.html and Google Earth, respectively.

Figure 2 Mean monthly temperature and precipitation between 2016 and 2017 (a) at Dajiuhu Wetland (31°28′50″N, 110°00′09″E, 1758 m a.s.l.; 10 km away from Congping Basin). Mean monthly temperature at Congping (blue line) was calculated based on the vertical lapse rate of temperature of 0.5°C/100 m. Anomalies in seasonal temperature (b) and precipitation (c) in the study area since 1880 were sourced from Wang and others (2009).

Figure 3 Particle size spectra and chronology of sediment cores in Congping (a) and Mulong (b), with mass accumulation rate (MAR, orange line) shown.

Figure 4 Diatom assemblages in Congping (a) and Mulong (b).

Figure 5 Fossil pigment diagrams of Congping (a) and Mulong (b).

Figure 6 Multiple proxies in sediment cores collected from Congping (a) and Mulong (b). Original and Suess effect corrected $\delta^{13}C$ values are indicated by filled circles and open squares, respectively.

Figure 7 Synthesis of sedimentary records (a-f) with (g) $\delta^{15}N$ (NO_3^-) and (h) nitrate concentration from the Summit, Greenland ice core (Geng and others 2014), (i) nitrate concentration from the Himalayan ice core (Thompson and others 2000), (j)

728 winter temperature anomalies based on reconstruction (Wang and others 2009).
729 Diatom PCA1 sample scores, pigment PCA1 sample scores, and $\delta^{15}N$ in Congping
730 (a, c, e) and Mulong (b, d, f) are shown.
731 **Figure 8** Biplots of redundancy analyses, main diatom species and significant variables
732 in CP (a) and ML (b), pigments and significant variables in CP (c) and ML (d).
733 Diatom species abbreviations: Bra bre: *B. brebissonii*, Cym gra: *Cymbella gracilis*,
734 Enc ces: *Encyonopsis cesatii*, Eun bil: *E. bilunaris*, Eun exi: *E. exigua*, Eun muc: *E.*
735 *mucophila*, Fru rho: *Frustulia rhomboides*, Gom par: *G. parvulum*, Han amp: *H.*
736 *amphioxys*, Nav cry: *N. cryptotenella*, Nei amp: *Neidium ampliatum*, Pin bor: *P.*
737 *borealis*, Pin mic: *P. microstauron*, Pin vir: *Pinnularia viridis*, Sel pup: *S. pupula*,
738 Sta ven: *S. construens* var. *venter*, Sta pho: *Stauroneis phoenicenteron*, Tab flo:
739 *Tabellaria flocculosa*.
740 **Figure 9** Schematic diagram of some possible effects of climate warming and nitrogen
741 deposition on primary producer communities. Effects of nitrogen deposition and
742 warming either inhibit (-) or stimulate (+) response variables.
743
744

	Congping	Mulong	Congping	Mulong
Sampling date	June 2016	June 2016	Sep. 2017	Sep. 2017
Latitude (N)	31°24′13.58″	31°24′10.03″	31°24′13.58″	31°24′10.03″
Longitude(E)	110°03′35.83″	110°03′17.89″	110°03′35.83″	110°03′17.89″
Altitude (m a.s.l.)	2073	2078	2073	2078
Water depth (m)	0.2	1.5	0.2	1.5
Secchi depth (m)	0.2	0.5	0.2	0.5
Area (m^2)	360	380	360	380
pH	6.17	5.17	6.43	5.83
Conductivity ($\mu S\ cm^{-1}$)	12	9	23	12
PO_4^{3-} ($\mu g\ L^{-1}$)	4	2	3	2
DOC ($mg\ L^{-1}$)	18.0	12.3	n.a.	n.a.
NO_3^- ($\mu g\ L^{-1}$)	73	22	115	25
K^+ ($mg\ L^{-1}$)	0.4	-	1.39	0.13
Ca^{2+} ($mg\ L^{-1}$)	1.04	0.86	1.22	0.69

Na^{+} (mg L^{-1})	0.71	0.26	0.78	0.07
Mg^{2+} (mg L^{-1})	0.27	0.19	0.25	0.12
Si (mg L^{-1})	0.17	0.43	0.87	0.52

-The value was below detection limit. n.a. Environmental factors were not measured.

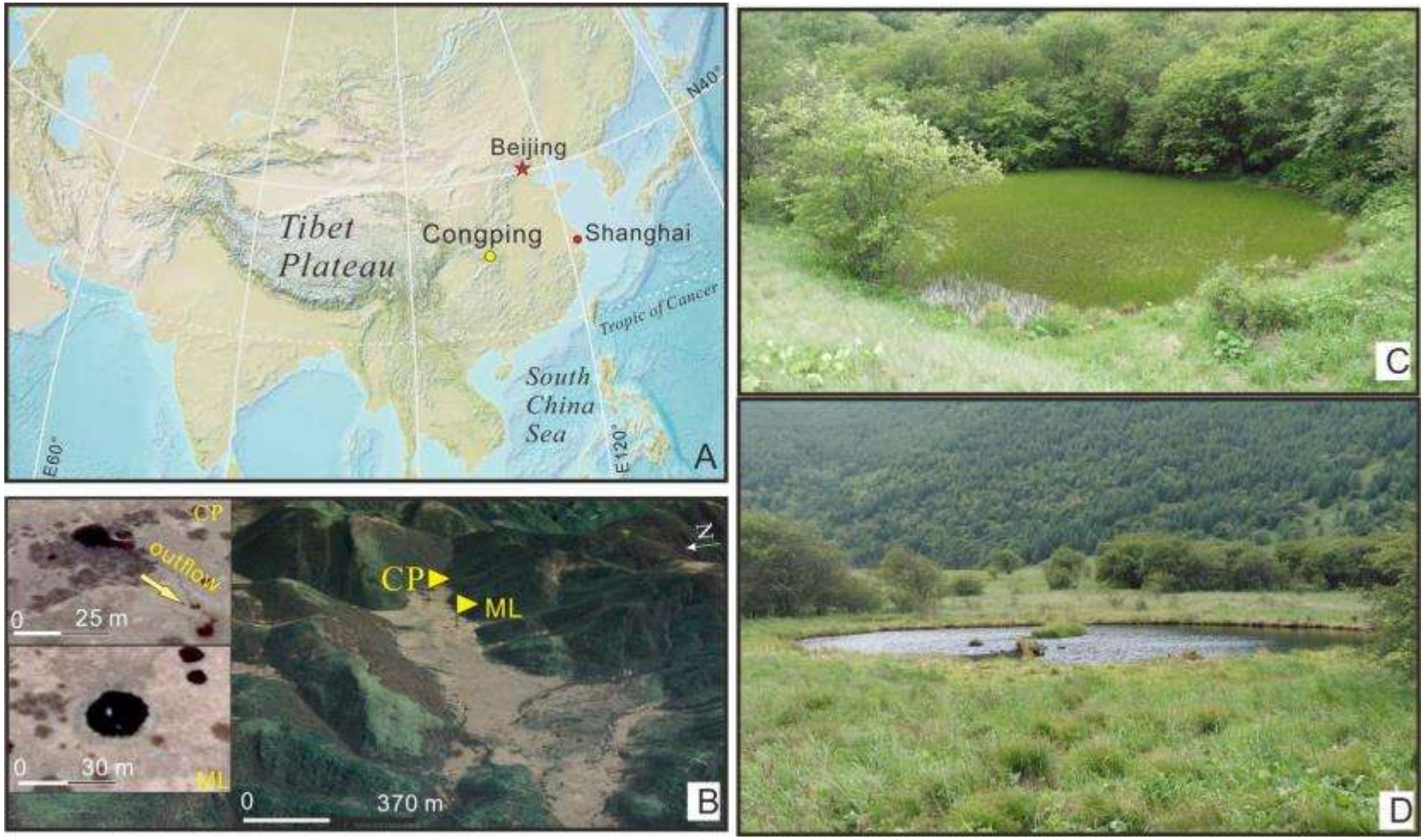
Beijing
Tibet
Plateau
Congping
Shanghai
Tropic of Cancer
South
China
Sea
N40°
E60°
E120°
A
CP
outflow
0
25 m
0
30 m
ML
CP
ML
N
0
370 m
B
C
D

Figure 1

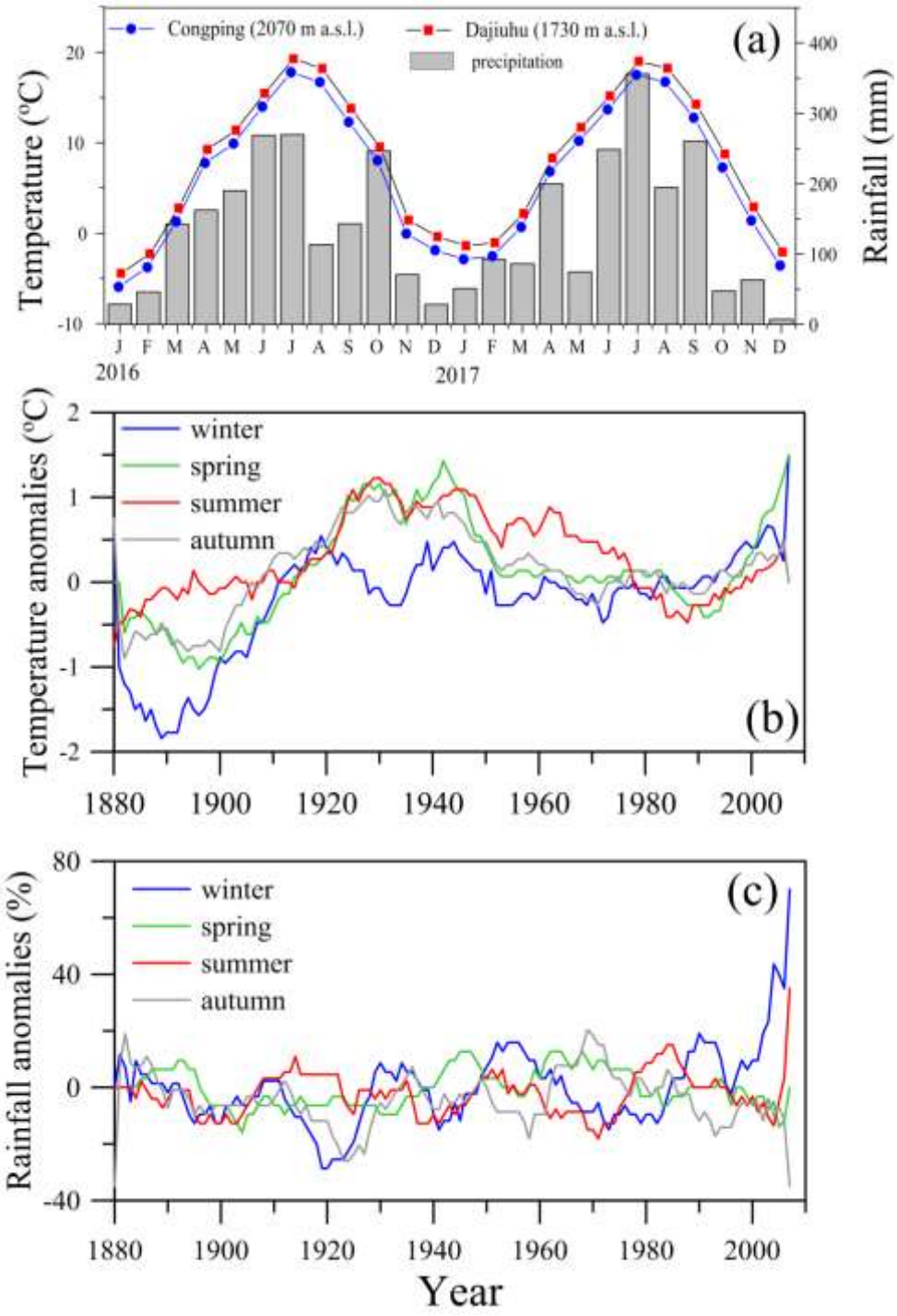
Congping (2070 m a.s.l.)
Dajiuhu (1730 m a.s.l.)
precipitation
(a)
Temperature (°C)
Rainfall (mm)
J F M A M J J A S O N D J F M A M J J A S O N D
2016
2017
Temperature anomalies (°C)
winter
spring
summer
autumn
(b)
1880 1900 1920 1940 1960 1980 2000
Rainfall anomalies (%)
(c)
Year

Figure 2

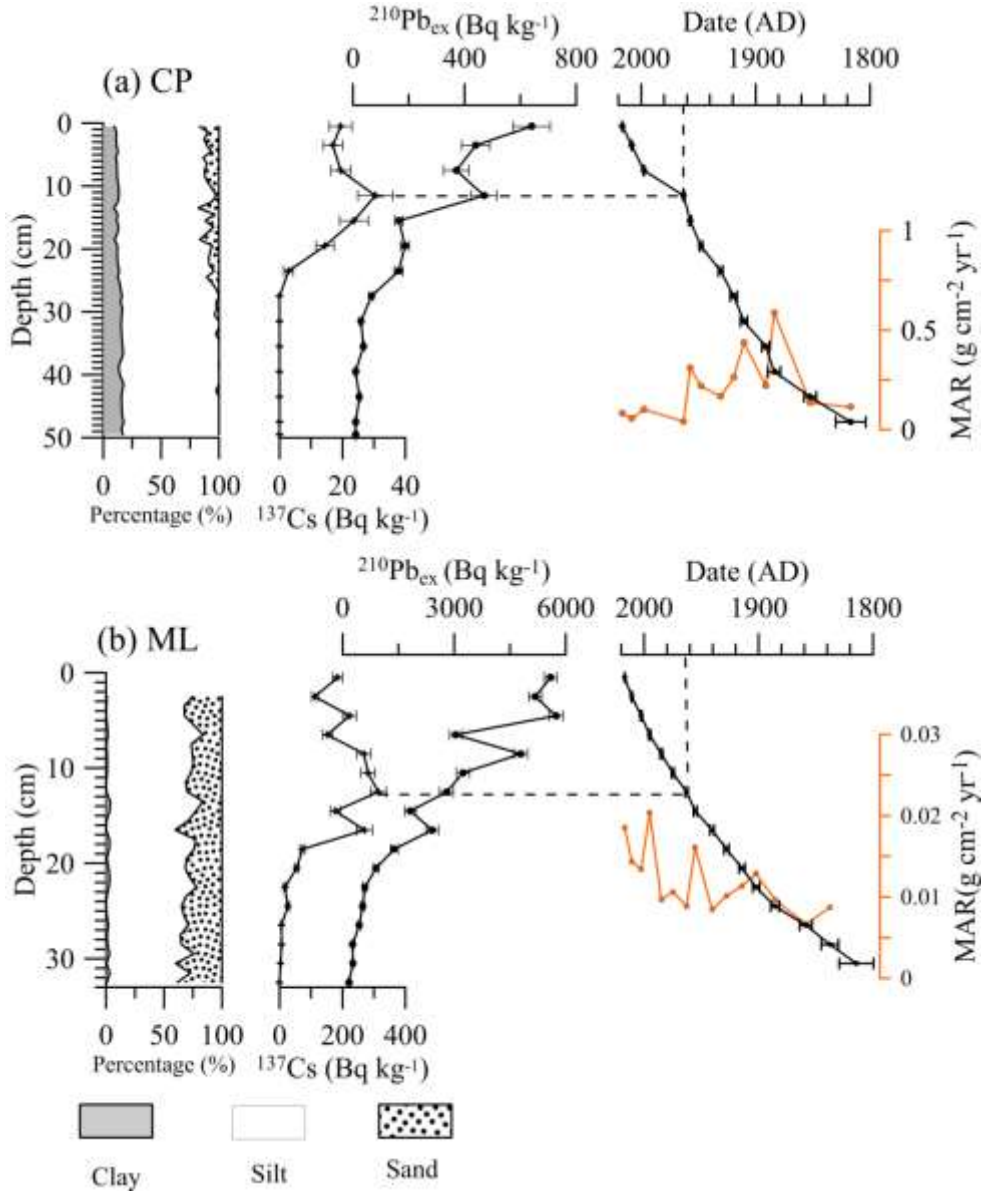
(a) CP
$^{210}Pb_{ex}$ (Bq kg^{-1})
Date (AD)
Depth (cm)
Percentage (%)
^{137}Cs (Bq kg^{-1})
MAR (g cm^{-2} yr^{-1})
(b) ML
Clay
Silt
Sand

Figure 3

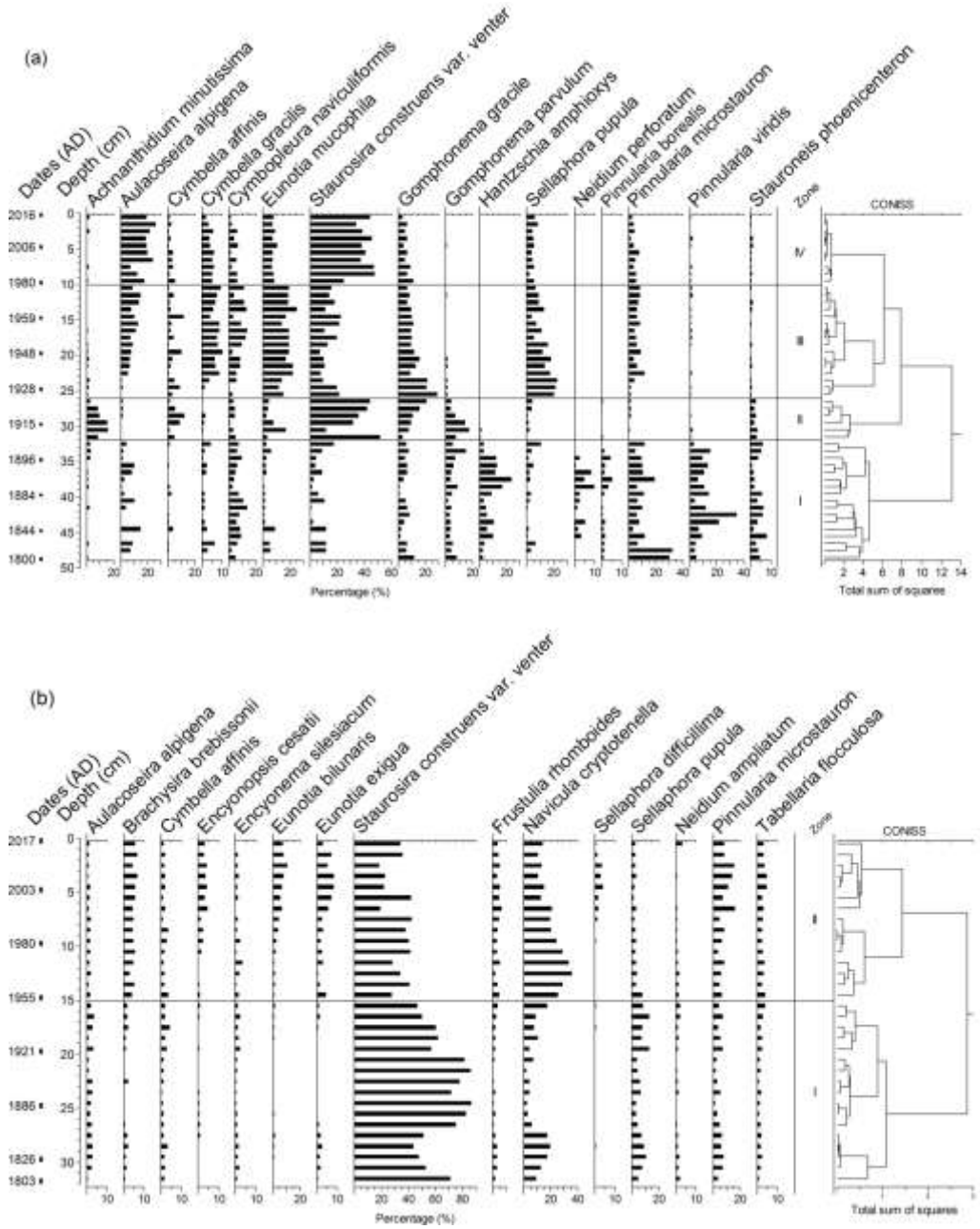
(a)
Dates (AD)
Depth (cm)
Achnanthidium minutissima
Aulacoseira alpigena
Cymbella affinis
Cymbella gracilis
Cymbopleura naviculiformis
Eunotia mucophila
Staurosira construens var. venter
Gomphonema gracile
Gomphonema parvulum
Hantzschia amphioxys
Sellaphora pupula
Neidium perforatum
Pinnularia borealis
Pinnularia microstauron
Pinnularia viridis
Stauroneis phoenicenteron
Zone
CONISS
Percentage (%)
Total sum of squares
(b)
Dates (AD)
Depth (cm)
Aulacoseira alpigena
Brachysira brebissonii
Cymbella affinis
Encyonopsis cesatii
Encyonema silesiacum
Eunotia bilunaris
Eunotia exigua
Staurosira construens var. venter
Frustulia rhomboides
Navicula cryptotenella
Sellaphora difficillima
Sellaphora pupula
Neidium ampliatum
Pinnularia microstauron
Tabellaria flocculosa
Zone
CONISS
Percentage (%)
Total sum of squares

Figure 4

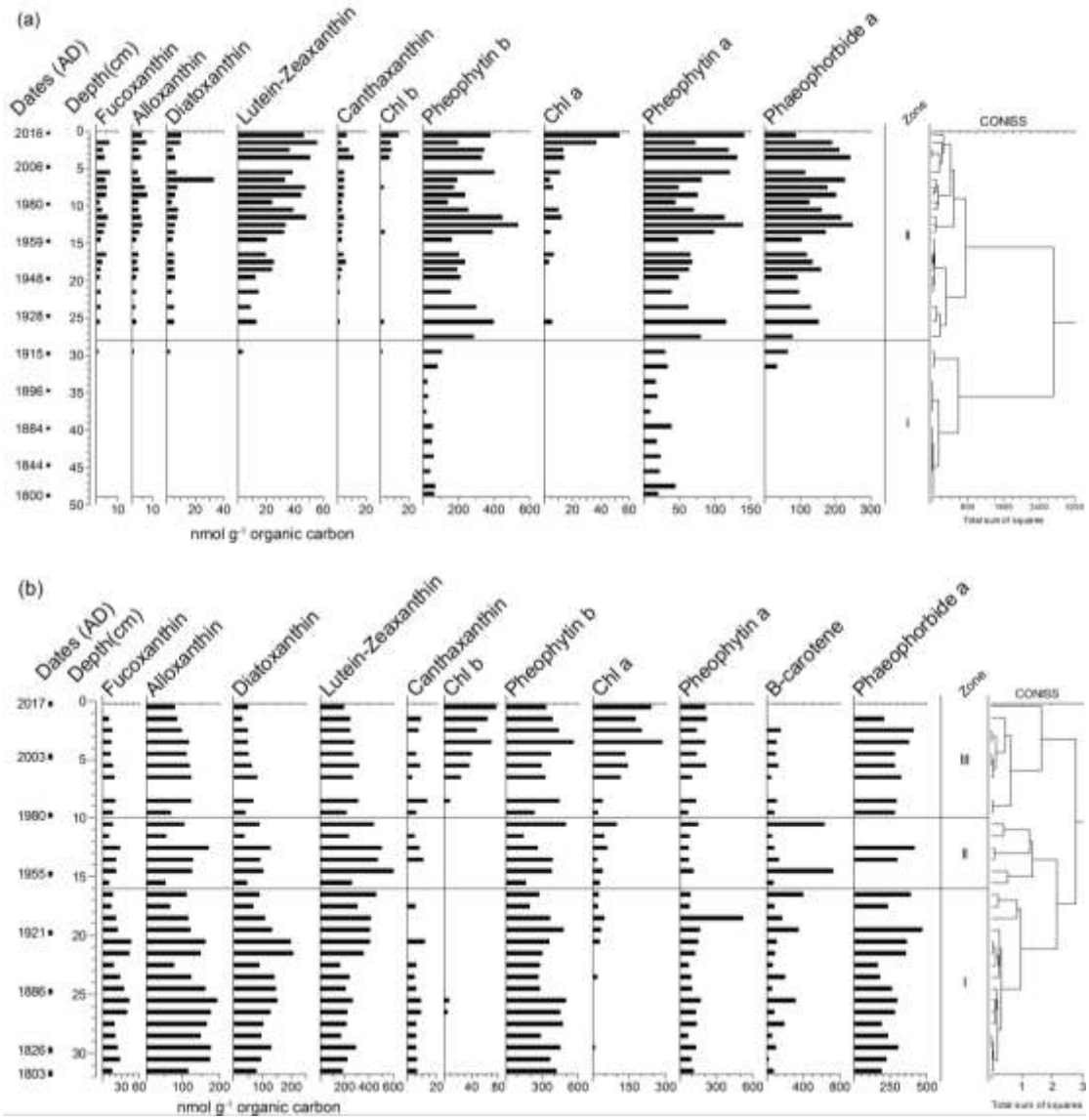
(a)
Dates (AD)
Depth(cm)
Fucoxanthin
Alloxanthin
Diatoxanthin
Lutein-Zeaxanthin
Canthaxanthin
Chl b
Pheophytin b
Chl a
Pheophytin a
Phaeophorbide a
Zone
CONISS
nmol g⁻¹ organic carbon
(b)
Dates (AD)
Depth(cm)
Fucoxanthin
Alloxanthin
Diatoxanthin
Lutein-Zeaxanthin
Canthaxanthin
Chl b
Pheophytin b
Chl a
Pheophytin a
B-carotene
Phaeophorbide a
Zone
CONISS
nmol g⁻¹ organic carbon

Figure 5

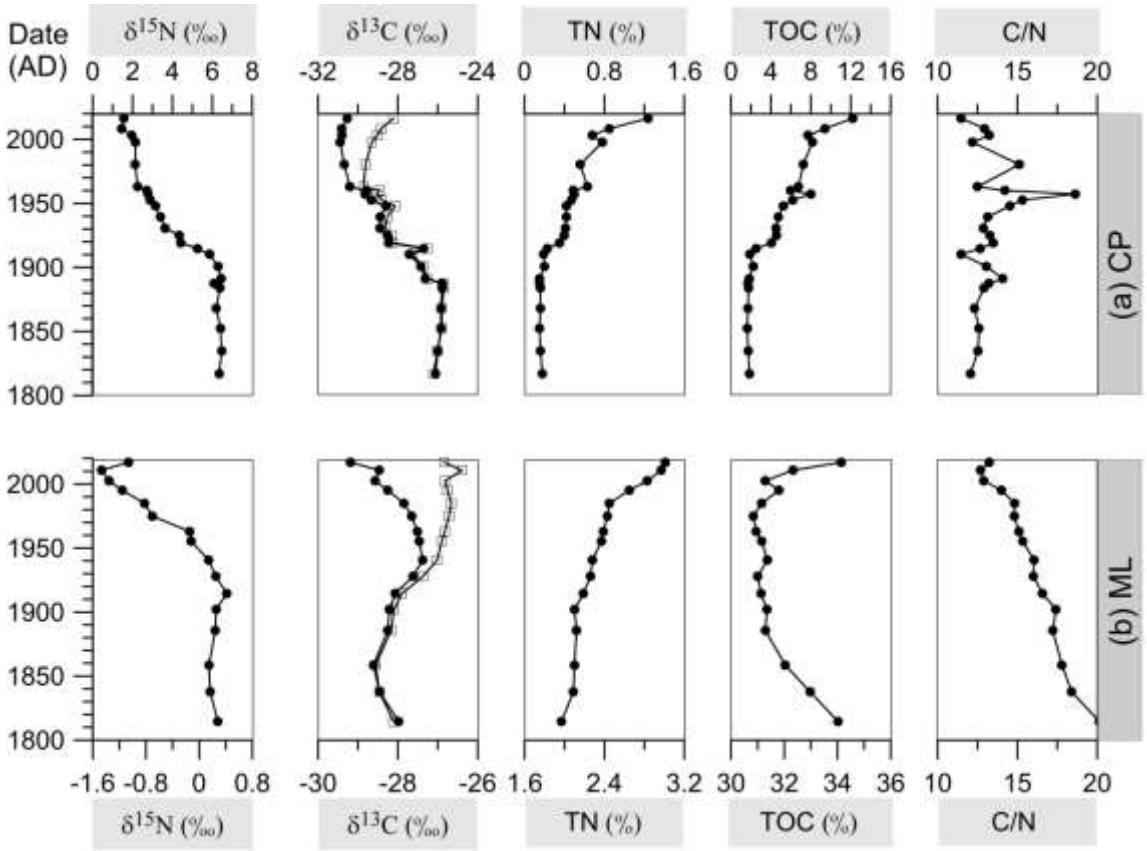
Date
(AD)
δ15N (‰)
δ13C (‰)
TN (%)
TOC (%)
C/N
0 2 4 6 8
-32 -28 -24
0 0.8 1.6
0 4 8 12 16
10 15 20
2000
1950
1900
1850
1800
(a) CP
(b) ML
-1.6 -0.8 0 0.8
-30 -28 -26
1.6 2.4 3.2
30 32 34 36
10 15 20

Figure 6

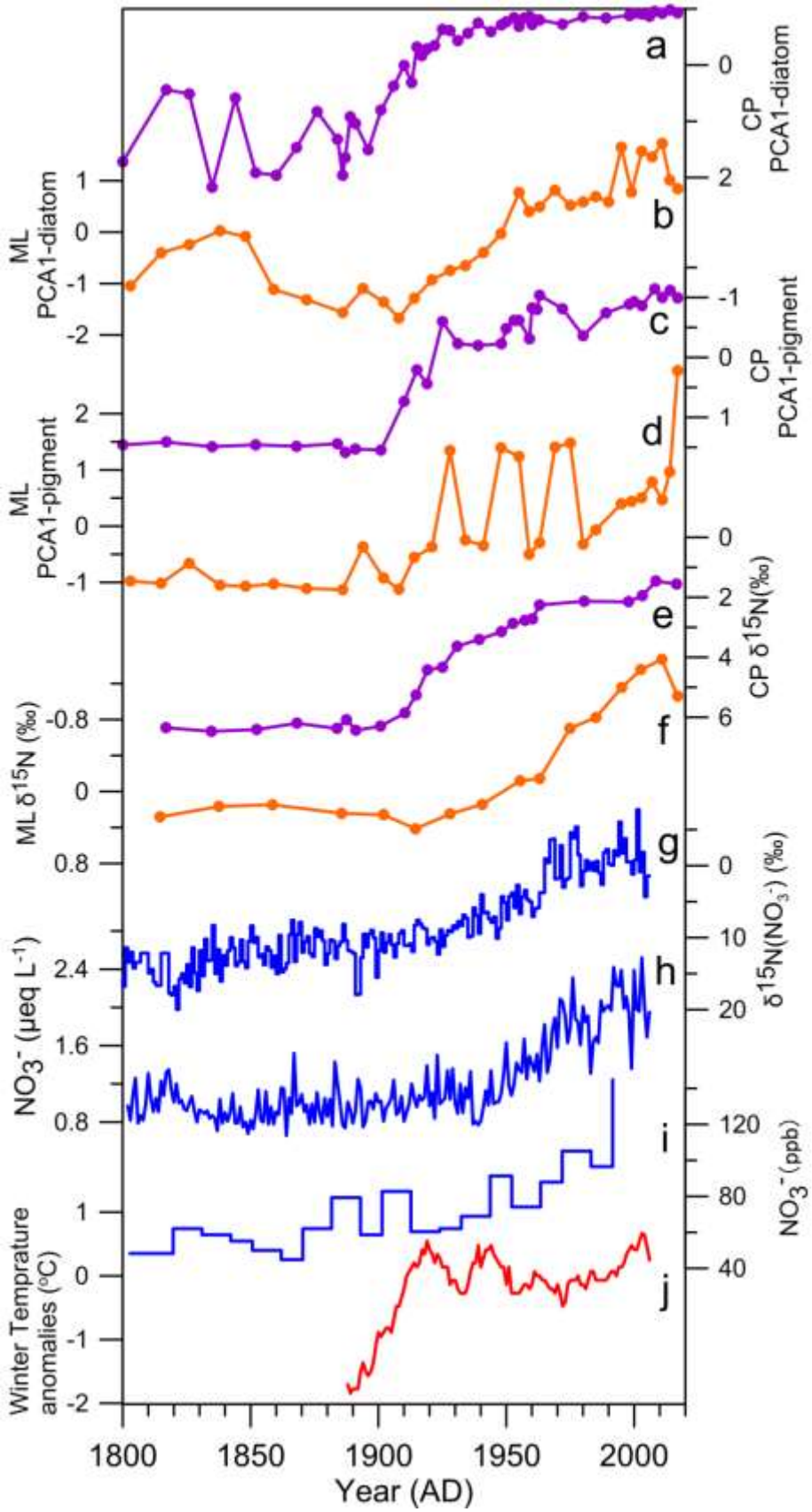
a
b
c
d
e
f
g
h
i
j
ML PCA1-diatom
CP PCA1-diatom
ML PCA1-pigment
CP PCA1-pigment
ML δ15N (‰)
CP δ15N(‰)
NO3- (μeq L-1)
δ15N(NO3-) (‰)
NO3- (ppb)
Winter Temprature anomalies (°C)
1800
1850
1900
1950
2000
Year (AD)

Figure 7

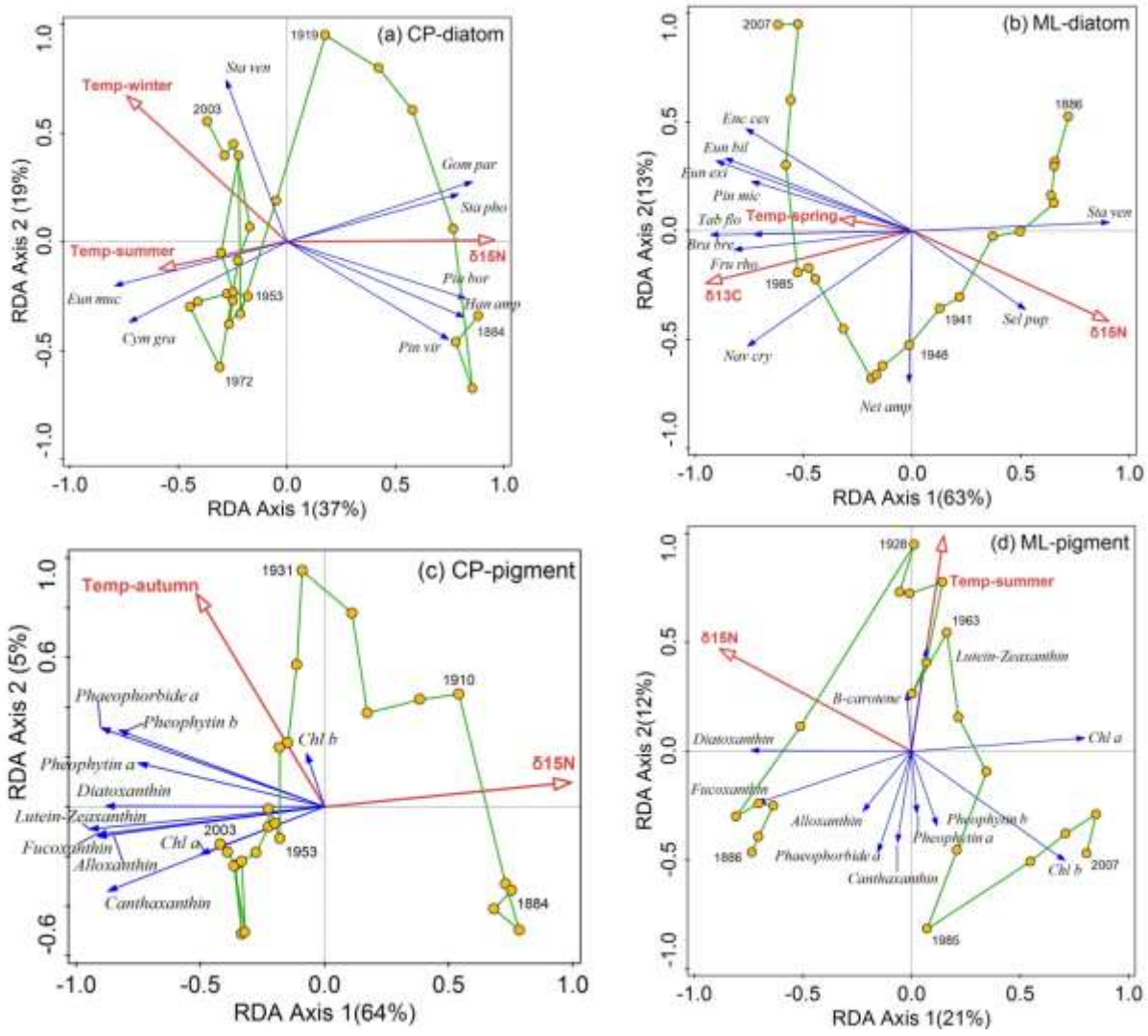
(a) CP-diatom
Temp-winter
Temp-summer
δ15N
Sta ven
Gom par
Sta pho
Pin hor
Han amp
Pin vir
Eun mac
Cym gra
1919
2003
1953
1884
1972
RDA Axis 2 (19%)
RDA Axis 1(37%)
(b) ML-diatom
Enc cev
Eun bil
Eun exi
Pin mic
Tab flo
Temp-spring
Bra bre
Fra rhu
δ13C
δ15N
Sta ven
Sel pup
Nav cry
Net amp
2007
1886
1985
1941
1946
RDA Axis 2(13%)
RDA Axis 1(63%)
(c) CP-pigment
Temp-autumn
δ15N
Phaeophorbide a
Pheophytin b
Pheophytin a
Diatoxanthin
Lutein-Zeaxanthin
Fucoxanthin
Alloxanthin
Chl a
Chl b
Canthaxanthin
1931
1910
2003
1953
1884
RDA Axis 2 (5%)
RDA Axis 1(64%)
(d) ML-pigment
Temp-summer
δ15N
Lutein-Zeaxanthin
β-carotene
Diatoxanthin
Chl a
Fucoxanthin
Alloxanthin
Pheophytin b
Pheophytin a
Phaeophorbide a
Canthaxanthin
Chl b
1928
1963
1886
2007
1985
RDA Axis 2(12%)
RDA Axis 1(21%)

Figure 8

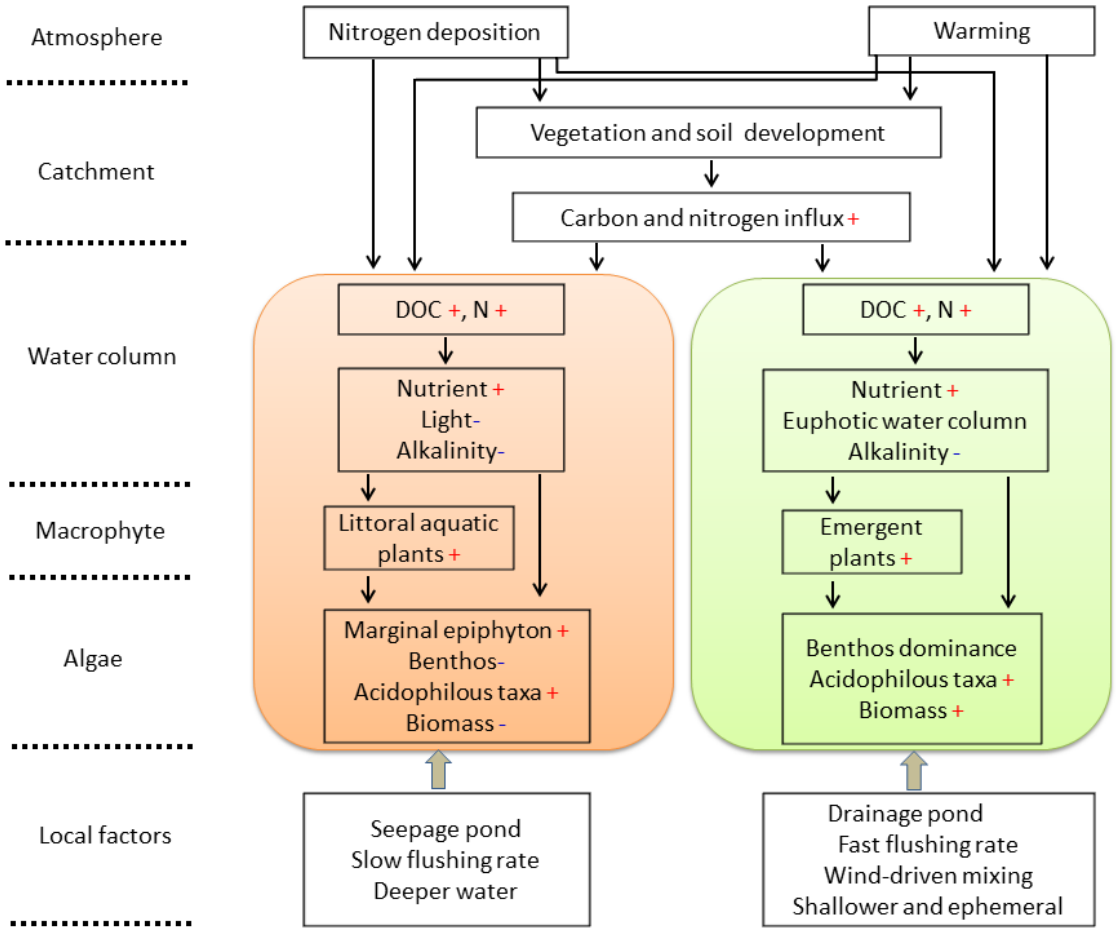
Atmosphere
Catchment
Water column
Macrophyte
Algae
Local factors
Nitrogen deposition
Warming
Vegetation and soil development
Carbon and nitrogen influx +
DOC +, N +
Nutrient +
Light-
Alkalinity-
Littoral aquatic plants +
Marginal epiphyton +
Benthos-
Acidophilous taxa +
Biomass -
DOC +, N +
Nutrient +
Euphotic water column
Alkalinity -
Emergent plants +
Benthos dominance
Acidophilous taxa +
Biomass +
Seepage pond
Slow flushing rate
Deeper water
Drainage pond
Fast flushing rate
Wind-driven mixing
Shallower and ephemeral

Figure 9